



24th COBEM - 2017



24th ABCM International Congress of Mechanical Engineering
December 3-8, 2017, Curitiba, PR, Brazil

COBEM-2017-1567

BEHAVIOR OF THE DISTRIBUTION OF LIFE IN NOTCHED COMPONENTS ACCORDING TO THEORY OF CRITICAL DISTANCE

Jéssica Nayara Dias

Jorge Luiz de Almeida Ferreira

Universidade de Brasília, Engineering Materials Integrity Program, FGA; Brasília, Brazil
jessicadias.engenharia@gmail.com, jorge@unb.br

Letícia Laleska Oliveira Silva

Universidade de Brasília, Mechanical Engineering Department, Brasília, Brazil
leticia.laleska@gmail.com

Abstract. *The Theory of Critical Distance (TDC) was reformulated to allow life prediction of notched components subjected to multiaxial loads. In this sense, as opposed to the classical approach, a fault function is used which contains information on the tensor of the stresses and/or deformations and admits that the characteristic length, L , varies with the fatigue life. Thus, it is proposed that the failure function is represented by the Smith-Watson-Topper parameter, SWT, in the critical plane. This is accomplished through the calibration and use of a critical distance curve, $L - N_f$, estimated based on the SWT parameter and subsequent application of critical plane search algorithms. In addition, for the quantification of life distribution behavior, the algorithms for estimating the $L - N_f$ curve and critical plane search were adapted for the use of the Monte Carlo simulation technique. For the validation of the model, a set of experimental data obtained from fatigue tests was used in specimens with and without notches made with the Al 7050-T7451 alloy, under uniaxial loads (push-pull and torsional) and multiaxial loads (torsion -traction). As results, it can be verified that the deterministic predictions of life presented a relatively good agreement when compared to the lives observed experimentally. From the analysis of the life results predicted by the Monte Carlo technique, it was possible to infer that the fatigue lives estimated under multiaxial loading conditions can be represented by lognormal or Weibull distributions, with greater adherence to the lognormal distribution. In addition, when comparing the life time related to the probabilities of failure of 2.5; 50 and 97.5% with the lives obtained experimentally, it was possible to observe that the upper limits are in a good concordance whereas the inferior ones present a significant difference in the region of confidence.*

Keywords: *fatigue, notched components, critical distance criterion, reliability, Monte Carlo*

1. INTRODUCTION

The presence of geometric discontinuities in engineering components is inevitable and these notches are considered a problem in the prediction of fatigue life (NICHOLAS, 2006; SUSMEL; TAYLOR, 2007; SOCIE, 1993). This defect produces a concentration of stresses that can bring the notched component to a fatigue behavior different from those not notched. Thus, it is considered that the notch represents a condition in which there are stress gradients ranging from the maximum stress, present at the root of the notch, to lower stresses located below it (NICHOLAS, 2006).

In the middle of the most used methods that consider the effect of stress gradients on the fatigue limit, we highlight those proposed by Neuber (1958) and Peterson (1959). According to the method proposed by Neuber (1958), known as the Theory of Critical Distance (TCD), the elastic stress in the stress concentrator does not present values as high as those that the mechanical theory of continuous means predicts. The actual stress that represents a real stress must be estimated close to the notch analyzed on units of materials (crystals, structural particles). Peterson (1959) proposes in his approach to analyze the material fatigue limit the reference stress should be calculated at a given distance from the apex of the stress concentrator (SUSMEL; TAYLOR, 2007).

The TCD have advantages over several other approaches since both the stress gradient and the effect of the size of the concentrator are addressed (NICHOLAS, 2006). In relation to notched components subject to multiaxial fatigue, the experimental data are relatively rare when compared to components without defects. However, there are many structures with the presence of notches subject to multiaxial loads, such as a combination of bending and torsion or traction and torsion (SOCIE, 1993). When evaluating the tension for this type of load, Wang (2014) states that it is

important to point out the differences between the invariant stress approaches and the critical planes. In order to characterize fatigue at the location of the stress concentrator in multiaxial fatigue, the size of the notch, shape, stress gradient, applied loads and phase should be considered (SOCIE, 1993).

In this article, the Smith-Watson-Topper (1970) - SWT model, is used to predict life in specimens subjected to multiaxial loading, in this model the plane of maximum normal deformation should be considered as the critical plane. This parameter is used for materials that have failed predominantly due to the growth of cracks in planes of maximum stress or deformation (WANG, 2014). In his work, Karakas (2013) stresses that this model is based on intrinsic properties of the material that are obtained from controlled fatigue tests.

In order that the deterministic and probabilistic predictions are performed for the life prediction of the components under study, the Monte Carlo simulation technique was used. The method realizes this prediction through the generation of random numbers, which will later return the expected value, in the case of this work, the component life forecast.

2. MULTIAXIAL MODEL AND LIFE DEPENDENT CRITICAL DISTANCE

2.1 The theory of critical distance (TCD)

This section briefly presents the critical distance theory (CARPINTERI, 2008; CASTRO, 2009; CICERO et al., 2012; SUSMEL, 2004; SUSMEL; TAYLOR, 2003, 2012; TAYLOR, 1999, 2008). The method aims to predict the fatigue strength of components with stress concentrators, such as notches or cracks (CASTRO, 2009). In TCD, fatigue failure is predictable when the effective stress in a process zone exceeds the fatigue resistance of the material. The reference stress can be found at a given point (point method, PM), or by averaging along a line (LM) or on an area (AM) or volume (VM) (SUSMEL; TAYLOR, 2003). The critical distance, represented by the characteristic length (L), varies for each method and can be calculated by:

$$L = \frac{1}{\pi} \left(\frac{\Delta K_{th}}{\sigma_0} \right)^2 \quad (1)$$

The equation shows that L depends on two characteristics: the fatigue resistance limit (σ_0) and the threshold value of the stress intensity factor for long cracks (ΔK_{th}). Castro (2009) showed that the size of the fatigue process zone depends on the assumed fatigue parameter. The volume is located around the notch, having a shape determined a priori and with one of the dimensions related to the material parameter. In this sense, the general expression representing this concept is presented in Eq. (2).

$$\frac{1}{V} = \int_V P(\sigma) dV \leq 0 \quad (2)$$

Where $\sigma \equiv (\sigma(x), t)$ is the history of the stress tensor at a point x located in the process zone of volume V , and $P(\sigma)$ is the function that defines the fatigue parameter.

For the estimation of critical distance based on the point method, for example, the function $P(\sigma)$ is defined by Eq. (3).

$$P(\sigma) := \sigma_{1a} - c \quad (3)$$

Where σ_{1a} is the maximum principal stress amplitude and c is a material parameter. Substituting the volume of the material in Eq. (2) by a point results in Eq. (4).

$$P(\sigma(l)) \leq 0 \quad (4)$$

In this specific case, Eq. (4) is evaluated at a distance l from the root of the notch. The parameter c can be obtained by applying Eq. (4) in the fatigue limit condition of a non-notched sample, in an experiment carried out under alternating loading conditions, obtaining:

$$c = \sigma_0 \quad (5)$$

Using Eq. (4) for a notched specimen tested under fatigue condition that failed in Mode I fracture, the equality shown in Eq. (6) is obtained.

$$l = 0.5L \quad (6)$$

However, in the construction proposed by Castro (2009), $\sigma(l)$ can be written as a function that contains information of the tensor of the tensions and/or deformation at a distance from the hot-spot - critical distance, and P defines the failure criterion by fatigue.

2.2 Extension of the TCD for fatigue life prediction

Susmel and Taylor (2007) reformulated the TCD by extending its application to predicting the fatigue life in the medium cycle. This extension is based on the hypothesis that the characteristic length, L , varies with the fatigue life according to the relation presented in Eq. (7). One of the possible methodologies used to obtain the constants A and b can be performed by calibrating the L versus N_f curve, in which it is necessary to use two S-N curves (One generated through tests of unnotched specimens and the other one generated by tests of notched specimens). Typically, this calibration is performed using the maximum principal stress amplitude, $\sigma_{I\alpha}$.

$$L(N_f) = AN_f^b \quad (7)$$

Where A e b are the material constants.

2.3 Application of the Smith-Watson-Topper multiaxial fatigue criterion in terms of TCD

The Smith-Watson-Topper model (1970) was developed to describe crack initiation modes ruled by normal deformation and stress to a material plane. Socie proposed the generality of the SWT parameter for multiaxial fatigue based on the concepts of critical plane (SOCIE, 1987, SOCIE; MARQUIS, 1999). In this model, it is assumed that the preferential plane for the propagation of the fatigue microcracks is the plane in which the energy density produced by the normal stress component passes through a maximum value. Thus, considering that the fault function representation presented in Eq. (4) can be written based on the maximum energy density of normal stress, under the specific fatigue conditions, the failure function will take the form of Eq. (8)

$$P(\sigma(l)) = \left(\frac{\Delta\varepsilon}{2} \sigma_{\max} \right)_{\max} - c(N) = 0 \quad (8)$$

Where $\frac{\Delta\varepsilon}{2}$ and σ_{\max} are respectively the normal strain amplitude and the maximum intensity of the normal stress vector acting in the plane of maximum normal energy density and $c(N)$ will be a parameter that varies with the life of fatigue. According to the relation presented in Eq. (9).

$$c(N) = A_{SWT} N_f^{b_{SWT}} \quad (9)$$

Where A_{swt} and b_{swt} are constants determined from fatigue tests.

The determination of the parameters of Eq. (9) can be obtained from fatigue tests on non-notched specimens (critical points on the surface of the test region). Thus, by substituting Eq. (9) into (8), it is possible to write Eq. (10), which expresses a function that correlates the maximum density of normal energy acting on the hot-spot with the number of cycles required to induce the failure due to fatigue in the specimen.

$$c(N_f) = P_{SWT} = \left(\sqrt{\frac{\Delta\varepsilon}{2} \sigma_{\max}} \right)_{\max} = A_{SWT} N_f^{b_{SWT}} \quad (10)$$

Once the behavior of the material parameter is defined as a function of the number of cycles, it will be possible to use a strategy similar to that proposed by Susmel and Taylor (2007) for the construction of the curve that correlates the critical distance based on the SWT parameter, L_{SWT} , with the life of notched specimens. In the strategy applied in this work, it is necessary to use, besides the P_{SWT} versus N curve, a curve representing the fatigue behavior of the material in the presence of the notch, respectively the elements (a) and (b) shown in Fig. (1). Once the range of life that is desired to estimate the L_{SWT} versus N curve is defined, for example: between $N1$ and $N2$, the remote stress level related to a given N_i life is calculated where a fault in the notched specimen was observed, finding the pair (N_i, S_{gross_i}) . The next step is to obtain the stress area in the region near the root of the stress concentrator (see Fig. (1.c)) and, from a critical plane identification and search algorithm, calculate the evolution of the maximum value of the SWT parameter in the

analyzed region, obtaining the P_{SWTmax} versus l curve (see Figure (1.d)). Once the P_{SWTmax} versus l curve is determined, a search process will be performed to identify the coordinate, l , where the value of the $P_{SWTmax}(l)$ function equals that of $P_{SWT}(N_i)$. This value represents a point (l_{SWT}, N) of the l_{SWT} curve versus N . To obtain the other points, the procedure above described must be repeated and, once the pairs (l_{SWT}, N) are obtained, the curve parameters can be estimated using non-linear regression techniques.

2.4 Deterministic prediction of fatigue life using the l_{SWT} versus N curve

In general, the life prediction methodology based on the l_{SWT} versus N curve does not differ from that proposed by Susmel and Taylor (2007) for that purpose of determining fatigue life of notched components subjected to complex multiaxial loads, the procedure is summarized below.

For the prediction of life, it is necessary to have the P_{SWT} versus N curve (which characterizes the behavior of the material) and the l_{SWT} versus N curve (which characterizes the behavior of the characteristic length, L , with the life of fatigue). Thus, considering a notched structural component subjected to a combination of external stresses, the life prediction will be obtained from the following steps developed specifically for the point method:

- Determine the tensile field near the notch root as shown schematically in Fig. (1.c).
- Assume hypothetically that the component life is N_{trial} and compute the critical distance $l_{SWT}(N_{trial})$;
- Estimate in the $l_{SWT}(N_{trial})$ position the SWT parameter value in the critical plane associated with the stress tensor located at that position, $P_{SWT}(N_{trial})$;
- It uses the P_{SWT} versus N and $P_{SWT}(N_{trial})$ curve, estimated in the previous step, to calculate the expected life value for the material, N_{SWT} ;
- If $|N_{trial} - N_{SWT}| \leq TOL$, it is assumed that the position of the critical distance has been found and the life of the structural component is N_{trial} . If not, select another life and return to step b).

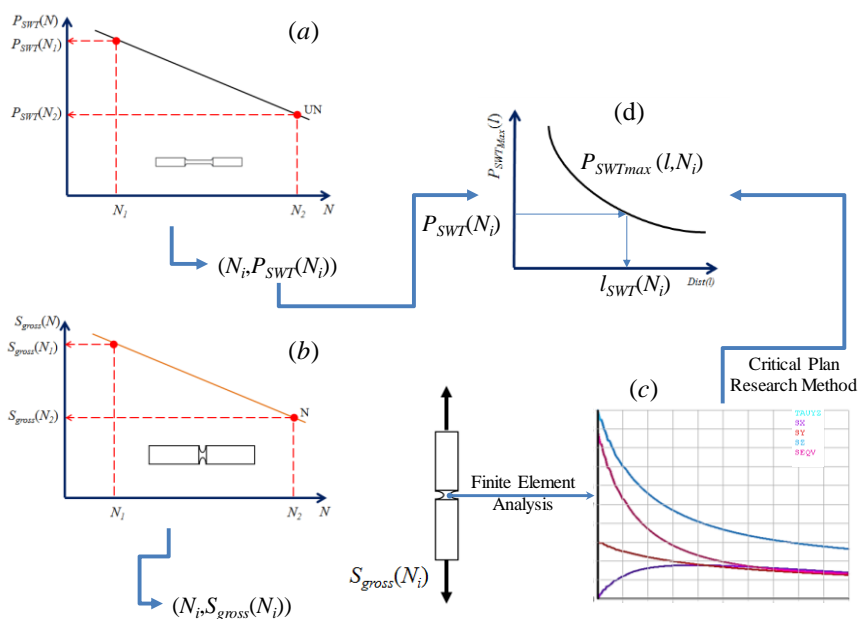


Figure 1. Representation of the basic structure for the characterization of the l_{SWT} versus N curve using the point method

3. APPLICATION OF THE MONTE CARLO METHOD IN THE CHARACTERIZATION OF FATIGUE LIFE DISTRIBUTION USING THE LIFE PREDICTION MODEL PROPOSED IN THIS WORK

Considering the sources of uncertainty, Monte Carlo simulation techniques were used to calculate the risks associated with the object under study. First, the problem was modified in order to present a probabilistic structure and the generated random numbers simulated the physical situation. In Monte Carlo simulation, the basic random variables in the limit state equation are generated randomly and used to estimate the probability of failure in the structure. In relation to the application of the fatigue method, it is considered n_a as the number of cycles in the simulation for which $g < 0$ in a total of N simulations. Thus, according to Ferreira (2006), one can estimate the probability of an unsatisfactory performance as:

$$P(g < 0) = \frac{n_a}{N} \quad (11)$$

Ferreira (2006) says that if p represents the probability of occurrence of the event where ($g < 0$), that is, $P(g < 0) = p$, then the inequality below is true for every positive value ε .

$$\text{Prob}\left[|F_a - p| \geq \varepsilon\right] \leq \frac{p(1-p)}{n\varepsilon^2} \quad (12)$$

The Monte Carlo simulation algorithm was constructed based on the deterministic fatigue life prediction structure using the l_{SWT} versus N curve, described in item 2.4. It was assumed that the sources of uncertainty that affect the life prediction are related to the material characterization curve, $P_{SWT} \times N$, and the curve that correlates the characteristic length behavior, L , with the fatigue life, l_{SWT} versus N . As a consequence, the constants and the exponent involved in the estimation of these curves will be considered random variables. Thus, It is considered that Eq. (13) to (15) control the fatigue life prediction process.

$$S_{gross}(N) = A_g N^{b_g} \quad (13)$$

$$P_{SWT}(N) = A_p N^{b_p} \quad (14)$$

$$l_{SWT}(N) = A_l N^{b_l} \quad (15)$$

It is emphasized that the parameters of Eq. (15) are obtained from Eqs. (13) and (14), following the procedure presented in item 2.4. For this reason, it was assumed that the parameters A_g , b_g , A_p e b_p , are primary random variables and that A_l e b_l will be evaluated dynamically during the life-prediction process.

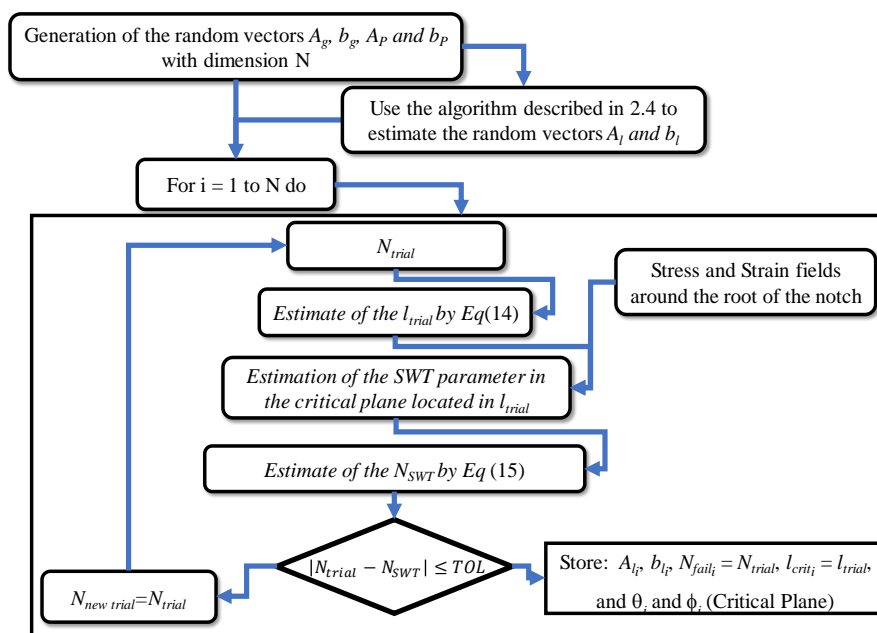


Figure 2. Flowchart summarizing the recursive procedure which can be used to estimate fatigue lifetime according to Monte Carlo Simulation

4. COMPARISON WITH EXPERIMENTAL DATA

Experimental results available by Sá (2017) will be used for the validation and analysis of the methodology proposed in this study. In Susmel and Taylor (2007) a study of fatigue behavior of Al 7050-T7451 alloy under multiaxial loading conditions is presented.

Table 1 reports the mechanical properties of the material and Fig. 3a presents the results of the fatigue uniaxial tests performed under and alternated torsion. This graph contains then the τ -N curves for the plain and for the notched specimens. In the case of the notched specimens (V-notched) these nominal stresses were computed in terms of the

gross area of the specimen. The Fig. 3.(b) has presented the curves P_{SWT} versus N (obtained from the experimental results realized with the specimens plain).

As outlined in ASTM E739 (1998), we consider that *the distribution of fatigue life (in any test) is unknown (and indeed may be quite complex in certain situations). For the purposes of simplifying the analysis (while maintaining sound statistical procedures), it is assumed in this practice that the logarithms of the fatigue lives are normally distributed, that is, the fatigue life is log-normally distributed, and that the variance of log life is constant over the entire range of the independent variable used in testing (that is, the scatter in log N is assumed to be the same at low S levels as at high levels of S).* In this sense, to obtain the parameters of the fatigue curves, the values of t and N obtained experimentally were linearized through the application of the logarithmic function and a linear regression process was performed. So, the trend line and the scatter bands sketched in these diagrams are characterized by a significance level equal to 95% (it was assumed, by hypothesis, that a lognormal distribution represents the number of cycles to failure). The synthesis of the generated results, carried out according to the above statistical procedure, is summarized in Table 2. In this table, $\log(A)$ and b represent the mean values of the Gaussian distribution, while the respective standard errors are related to the standard deviations. Table 3 summarizes the parameters of the P_{SWT} versus N curve, estimated using a linear regression technique.

Table 1. Mechanical Properties of Alloy Al 7050-T7451.

σ_v (MPa)	σ_u (MPa)	E (GPa)
453	513	73

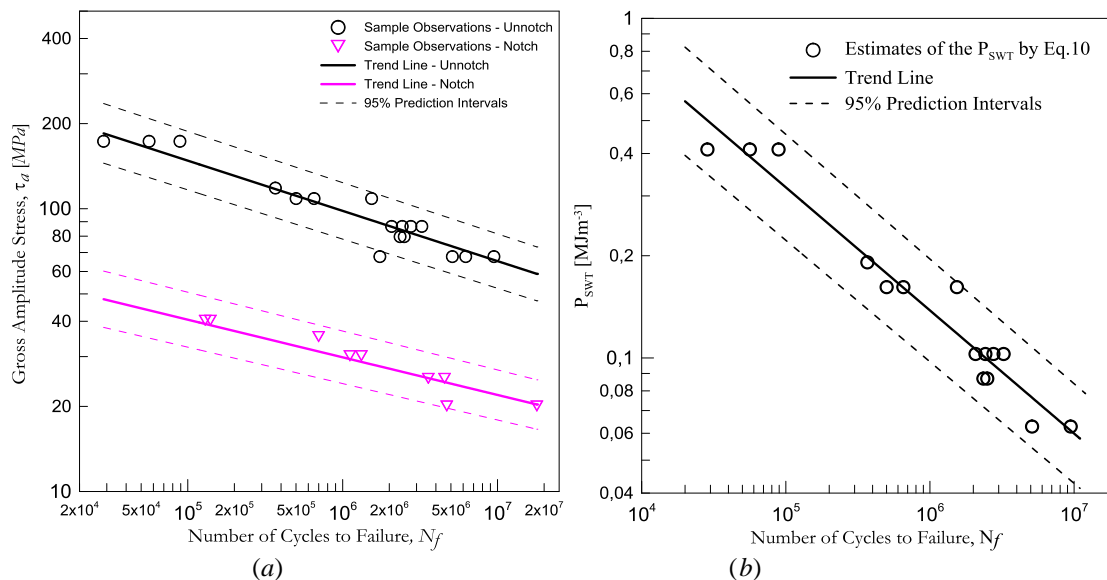


Figure 3. Fitted Relationship Between the (a) Fatigue Life, N , and Torsional stress, τ , of plain and notched specimens, (b) Fatigue Life, N , and P_{SWT} (performed under torsion conditions)

4.1 Fatigue life estimate in notched components tested under Push-Pull Conditions

In this first part of the methodology validation process, experimental results obtained by Sá (2017) were used in conditions of traction and compression (Push-Pull). In order to make a fair comparison between the results, the diagram $S-N$ representing the behavior of notched specimens subjected to push-pull conditions is shown in Fig. 4. In the diagram $S-N$, circular marks and continuous black lines respectively represent the experimentally observed results and the frontiers of the prediction interval of the individual values of σ_g (dependent variable) estimated from the linear regression procedures of the experimental data in the domain Log-log. The diamond marks represent the life values calculated using the methodology described in section 2.4 (deterministic prediction), while the crosses and the solid blue lines present the median and the limits of the confidence interval of the distribution of the fatigue lives obtained at methodology described in section 3 (Monte Carlo method). Comparing the values of life observed experimentally with those predicted by the deterministic model it is observed that, in general terms, the predicted lives are higher than those observed experimentally. However, considering the dispersion of the experimental results and the range of the prediction interval of the individual values of σ_g , it is quite reasonable to admit that the differences between the observed experimentally and estimated lifetimes by the deterministic model are statistically similar. The confidence interval of the fatigue life distribution obtained by Monte Carlo simulation was calculated assuming that the fatigue life distribution follows a lognormal distribution. This hypothesis was validated by scoring the life distributions for the

stress levels used in the tests (Fig. 5 (a)) and subsequent construction of the respective p-p diagrams (Fig. 5 (b)). Thus, from the analysis of the p-p diagrams, it could be verified that the estimated lives by Monte Carlo simulation can be represented by the lognormal distribution.

Table 2. Results of linear regression generated under torsion loading for plain and V-notched specimens.

Specimen Type	Number of Data	Parameter of the S-N curve			
		$\text{Log}(A)$	Std. Error	b	Std. Error
Plain	17	3,113	0,092	-0,187	0,150
V-notched	9	2,415	0,015	-0,155	0,017

Table 3. Synthesis of the parameters of the P_{SWT} versus N (Experimental data obtained under torsional tests on plain specimens)

Parameters	Unstandardized Coefficients	
	Mean	Std. Error
$\text{Log}(A_p)$	1,315	0,142
b_n	-0,362	0,024

Assuming that the lives obtained by Monte Carlo simulation are described by means of lognormal distributions, it was possible to define the lives related to failure probabilities equal to 2.5, 50 and 97.5%. From the failure levels of 2.5 and 97.5% the boundaries of the confidence interval of the life forecasts, represented by the blue lines, were plotted. However, the lives related to the failure level of 50% were used to identify the median life expectancy of the trials, represented in Fig. 4 by the crosses. Comparing these three measures of position of life distributions, it can be verified that: i) the lives predicted by the deterministic model are directly related to the median life expectancy of the specimens tested (all diamonds are superimposed on the crosses); ii) there is a relatively good agreement for the upper limits of the region of confidence; iii) there is a significant difference between the lower limits of the confidence regions predicted by the linear regression technique and by Monte Carlo simulation. Probably such behavior can be explained by the fact that the linear regression model used assumes that the parameters that characterize the S-N curve are intrinsically related to the Gaussian distribution (domain varies between $\pm\infty$), in contrast to life obtained by simulation of Monte Carlo, which showed a behavior well represented by the lognormal distribution, which is asymmetric with domain ranging from $0 < N < +\infty$.

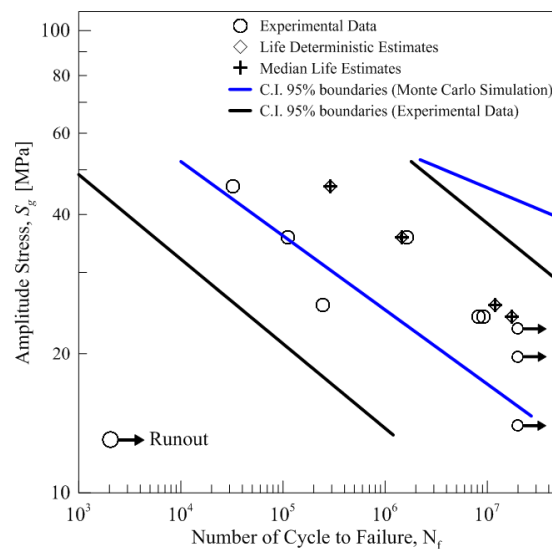


Figure 4. Fatigue results generated under fully loading and Monte Carlo Simulation

4.2 Fatigue life estimate in notched components tested under multiaxial loading conditions

The experimental program considered two ratios between the normal and shear nominal stress amplitudes (column (c), in Table 5). Eight tests were conducted using the first ratio and seven for the latter one. The actual lives are reported in column (d) of Table 3. The estimated lives considering procedure present in section 2.4 are presented in columns (e). Graphically, the quality of the results of such estimates can be assessed by plotting the actual lives against the predicted

ones, as shown in Fig. 6. In such graph, the continuous lines parallel to the one passing through the origin and the dashed lines represent bandwidths by factors of 2 (blue) and 4 (red), respectively. It can be seen from Fig. 6 that the proposed model provided fairly satisfactory predictions of life, since about 90% of the estimates are in the range related to the factor of 4, while about 50% of the estimates are in the range related to the factor of 2. In addition, 2 of 15 results provided non-conservative estimates of life.

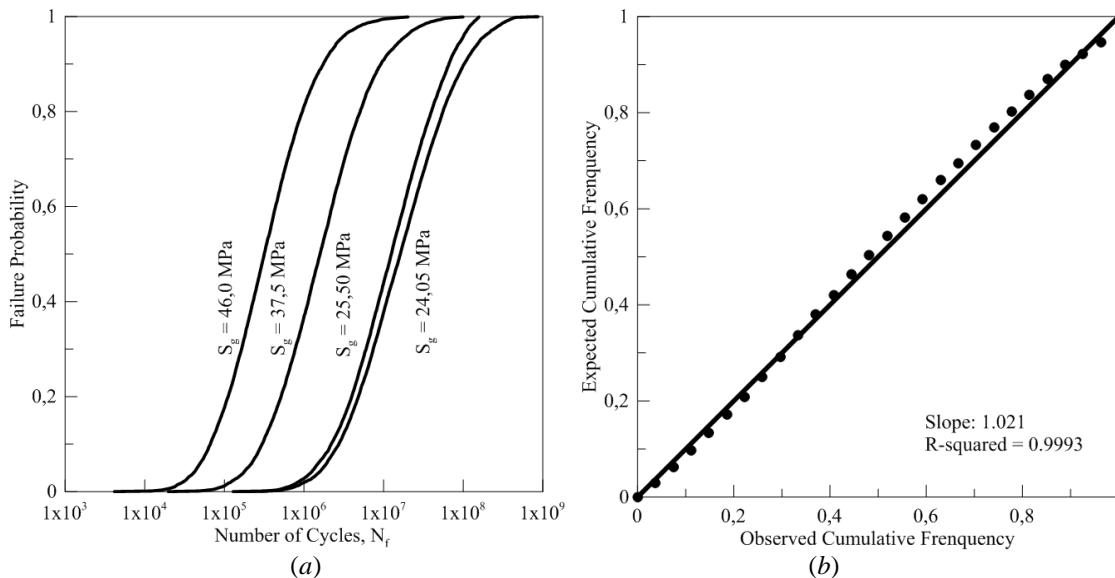


Figure 5. (a) Estimates of Fatigue Life Distributions and (b) Typical behavior of the P-P diagram of the fatigue life distribution (Theoretical Distribution: Lognormal).

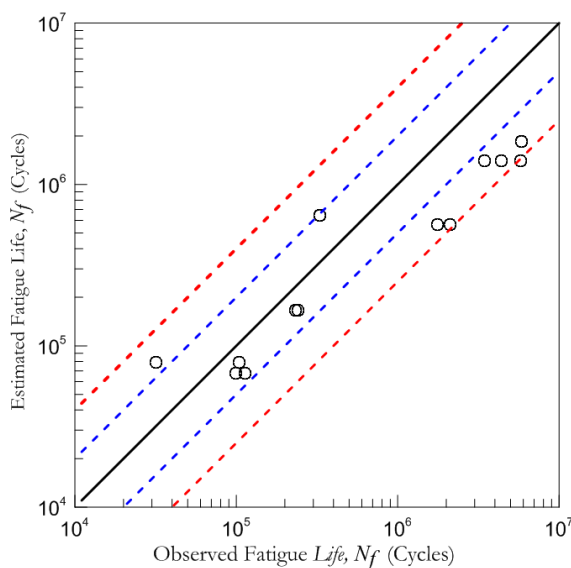


Figure 6. Observed versus estimated lives based methodology present on section 2.4.

The study of the probabilistic behavior of fatigue life predictions will be concentrated in the tests carried out with σ_g equal to 16 MPa and τ_g equal to 20 MPa. For this analysis, a sample set was generated with 10.000 stochastic predictions. With the sample set, an analysis was performed on the probability distribution function that best represents the behavior of the generated data. The lognormal distribution and the Weibull distribution were the ones that best represented the sample set of all the tested distributions. In Fig. 7 the P-P diagram resulting from these analyses is presented. It can be noted that the lives generated by the Monte Carlo technique have a greater adherence to the lognormal distribution than the Weibull distribution. However, since the Weibull distribution is typically used to represent fatigue life behavior, it will be maintained in the analysis.

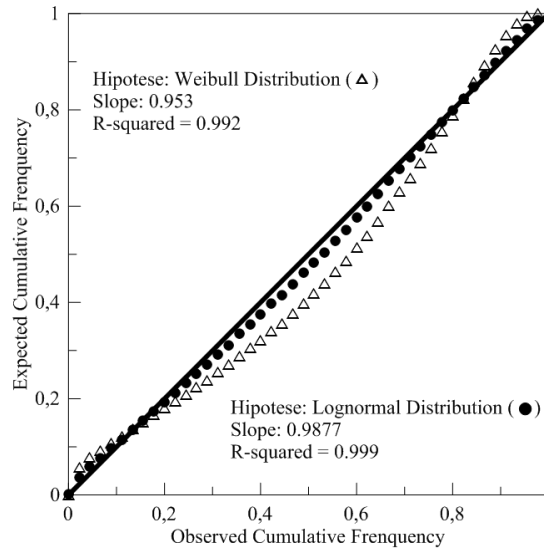


Figure 7: P-P diagram of the fatigue life distribution

In Fig. 8 the estimates of the cumulative probability distribution of the fatigue life for the situation of the notched specimens subjected to stresses $\sigma_g = 16$ MPa e $\tau_g = 20$ MPa are presented. The analysis of this figure allows to verify that the hypothesis of the sample distribution is described by the lognormal distribution is significant, since both the results obtained experimentally and the deterministic prediction of life are positioned exactly on the curve that represents this distribution. It is also noted that the curve representing the Weibull distribution, despite having a relatively high adhesion when considering the P-P diagram shown in Fig. 7, does not allow to consistently represent the behavior of the points related to the experimental data and estimated by the deterministic model.

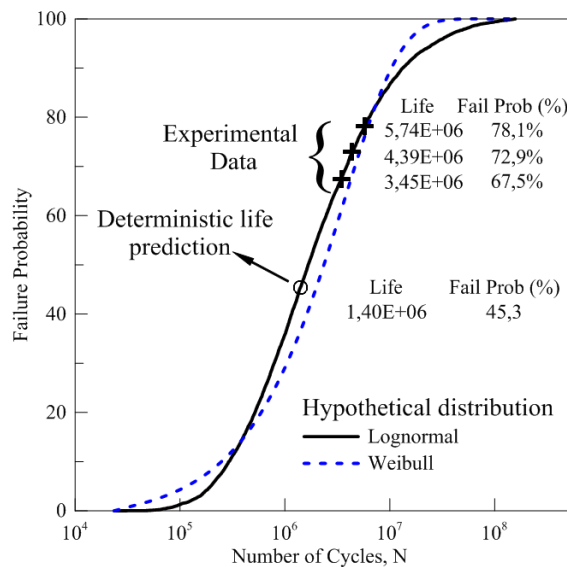


Figure 8: Estimating the cumulative probability distribution of the fatigue life of the carved specimens subjected to the loading conditions: $\sigma_g = 16$ MPa and $\tau_g = 20$ MPa

5. CONCLUSIONS

Using as a parameter of comparison the lives obtained by Sá (2017) under conditions of traction and compression (Push-Pull) it was possible to observe that the life predictions calculated in this work, (lswt versus N) is relatively higher for notched specimens subjected to multiaxial loads. However, this result is attenuated considering that the experimental results have been dispersed and the individual values of σ_g are predicted over a given interval. Through the Monte Carlo simulation, it was possible to validate the hypothesis that the distribution of fatigue life follows a lognormal distribution. In this configuration, with the comparison of related lives the failure probabilities of 2.5, 50 and 97.5% with the lives obtained experimentally, it was possible to observe that the higher limits are in a good agreement

while the lowers ones present a significant difference in the confidence region.

For the loading conditions studied (σ_g , τ_g), the life prediction using the proposed model compared to a life obtained through tests for the multiaxial fatigue data generated from V-notched specimens presented satisfactory values. The distribution that best fit the sample set used to determine the probabilistic behavior of the fatigue life predictions for the tests with σ_g equal to 16 MPa and τ_g equal to 20 MPa, for a lognormal distribution and the Weibull. However, a lognormal distribution is better suited for both the experimental results and the deterministic predictions.

6. REFERENCES

- ASTM E739-91, 1998. "Standard Practice for Statistical Analysis of Linear or Linearized Stress-Life (S-N) and Strain-Life (ϵ -N) Fatigue Data".
- Carpinteri, A., et al., 2008. "A multiaxial criterion for notch high-cycle fatigue using a critical-point method". *Engineering Fracture Mechanics*, Parma Italy, Vol. 75, n. 7, p.1864-1874.
- Castro, F. C.; Araújo, J. A.; Zouain, N., 2009. "On the application of multiaxial high-cycle fatigue criteria using the theory of critical distances". *Engineering Fracture Mechanics*, Brasília DF, Vol. 76, n. 4, p.512-524.
- Cicero, S.; Madrazo, V.; Carrascal, I.A., 2012. "Analysis of notch effect in PMMA using the Theory of Critical Distances". *Engineering Fracture Mechanics*, Cantabria, Spain, Vol. 86, p.56-72.
- El Haddad, M. H.; Topper, T. H.; Smith, K. N.: Prediction of non propagating cracks. *Engineering Fracture Mechanics*, 11, (1979), 573-584.
- Ferreira, J. L. A. et al., 2006. "Fatigue Reliability Assessment of a Kaplan Hydro Turbine Blade Under Cyclic Load". In: *IV Congresso Nacional de Engenharia Mecânica*, 2006, Recife. Anais do IV Congresso Nacional de Engenharia Mecânica. p. 1-10
- Karakas, Özler., 2013 "Consideration of mean-stress effects on fatigue life of welded magnesium joints by the application of the Smith–Watson–Topper and reference radius concepts". *International Journal of Fatigue*, Denizli, Turkey, Vol. 49, p.1-17.
- Neuber H., 1958. *Theory of notch stresses*. Berlin: Springer.
- Nicholas, T., 2006. "High Cycle Fatigue: A Mechanics of Materials Perspective". Ohio, USA: *Elsevier*.
- Peterson R. E., 1959. "Notch sensitivity". In: Sines G, Waisman JL, editors. *Metal fatigue*. New York: McGraw Hill. p. 293–306
- Sá, M. V. C; Ferreira, J.L.A.; Silva, C.R.M., Araújo, J.A., 2017. "Notched multiaxial fatigue of Al7050-T7451: on the need for an equivalent process zone size". *Frattura ed Integrità Strutturale*, DOI: 10.3221/IGF-ESIS.tt.uu.
- Smith, R.N., Watson, P. & Topper, T.H., 1970. "A stress-strain parameter for the fatigue of metals". *Journal of Materials*, 5(4), pp. 767–778.
- Socie, D., 1987. "Multiaxial fatigue damage models". *Journal of Engineering Materials and Technology*, 109, 292-298.
- Socie, D., 1993. "Critical Plane Approaches for Multiaxial Fatigue Damage Assessment, Advances in Multiaxial Fatigue". ASTM STP 1191, McDowell, D.L. and Ellis, R. (eds). pp. 7–36, *American Society for Testing and Materials*, Philadelphia
- Socie, D. F.; Marquis, G. B., 1999. "Multiaxial Fatigue". Warrendale, United States: SAE International. 502 p.
- Susmel, L., 2004. "A unifying approach to estimate the high-cycle fatigue strength of notched components subjected to both uniaxial and multiaxial cyclic loadings". *Fatigue & Fracture of Engineering Materials & Structures*, Vol. 27, n. 5, p.391-411.
- Susmel, L.; Taylor, D., 2003. "Two methods for predicting the multiaxial fatigue limits of sharp notches". *Fatigue & Fracture Engineering Materials & Structures*, Vol. 26, n. 9, p.821-833.
- Susmel, L.; Taylor, D., 2007. "A novel formulation of the theory of critical distances to estimate lifetime of notched components in the medium-cycle fatigue regime". *Fatigue & Fracture Of Engineering Materials And Structures*, Vol. 30, n. 7, p.567-581. Wiley-Blackwell.
- Susmel, L; Taylor, D., 2012. "A critical distance/plane method to estimate finite life of notched components under variable amplitude uniaxial/multiaxial fatigue loading". *International Journal of Fatigue*, Vol. 38, p.7-24.
- Taylor, D., 1999. "Geometrical effects in fatigue: a unifying theoretical model". *Int J Fatigue*, 21 pp. 413–20
- Taylor, D., 2008. "The theory of critical distances. *Engineering Fracture Mechanics*", Vol. 75, n. 7, p.1696-1705.
- Wang, L. et al., 2014. "Evaluation of multiaxial fatigue life prediction criteria for PEEK". *Theoretical and Applied Fracture Mechanics*, Vol. 73, p.128-135.

7. RESPONSIBILITY NOTICE

The authors Jéssica Nayara Dias, Jorge Luiz de Almeida Ferreira and Letícia Laleska are the only responsible for the printed material included in this paper.